Conditioning Medicine
www.conditionmed.org

REVIEW ARTICLE | OPEN ACCESS

Using ^{13}C hyperpolarized magnetic resonance spectroscopy to identify novel metabolic targets for preventing cardiac disease

Shuo Cong[1-3*], Xiao Meng Wang[2*], Chrishan J.A. Ramachandra[1,2] Derek John Hausenloy[1-5#]

Heart failure (HF) is one of the leading causes of death and disability worldwide, and new treatments are needed to prevent the onset and progression of this debilitating condition. Metabolic perturbations are known to underlie many cardiac diseases that result in HF, including acute myocardial infarction (AMI) and cardiomyopathies resulting from diabetes or hypertension. The emergence of ^{13}C hyperpolarized magnetic resonance spectroscopy (HP MRS) provides an innovative strategy for assessing in vivo metabolic flux in the diseased heart and has provided unique insights into the pathophysiology of AMI and diabetic and pressure-overload cardiomyopathies. Initial clinical studies have demonstrated the feasibility of using this metabolic imaging approach in patients with cardiac disease including AMI and diabetic cardiomyopathy. In this article, we provide an overview of the role of HP MRS in elucidating the in vivo metabolic perturbations underlying cardiac disease, and highlight potential therapeutic targets and strategies for modulating cardiac metabolism that may be adopted to improve outcomes in patients at risk of developing HF.

Keywords: ^{13}C hyperpolarized magnetic resonance spectroscopy, metabolic probes, cardiac disease, acute myocardial infarction, heart failure

Introduction

Heart failure (HF) is one of the leading causes of death and disability worldwide. As such, new treatments are needed to prevent the onset and progression of HF in order to improve health outcomes in patients with cardiac disease. Crucially, metabolic perturbations underlie several forms of cardiac disease including ischemic heart disease, diabetic cardiomyopathy, dilated cardiomyopathy, hypertrophic cardiomyopathy, anthracycline cardiomyopathy, peripartum cardiomyopathy, and mitochondrial cardiomyopathies, which ultimately leads to HF (Karwi et al., 2018; Ramachandra et al., 2019; Ramachandra et al., 2021). The clinical implementation of innovative strategies that can provide novel insight into these metabolic disturbances may help to identify new metabolic targets for improving clinical outcomes.

Positron emission tomography (PET) and magnetic resonance spectroscopy (MRS) are two methods currently used in clinical practice to evaluate the metabolic profile of patient hearts. PET offers high molecular specificity and sensitivity in imaging glucose, amino acids, and fatty acids (Labbe et al., 2012); however, the use of ionizing radiation limits its application to repeated or longitudinal imaging (Ntziachristos et al., 2019). Alternatively, conventional MRS (e.g., ^{31}P-MRS), though capable of accurately acquiring spatial information, is unable to assess metabolic flux. The advent of dynamic nuclear polarization (DNP) and its derived hyperpolarized (HP) MRS (Ardenkjaer-Larsen et al., 2003; Golman et al., 2006) has dramatically increased the sensitivity for detection of ^{13}C-labeled molecules, allowing the assessment of metabolic flux, which provides a significant advantage over early stage ^{13}C-MRS, the latter impeded by low signal-over-noise sensitivity (Shulman et al., 1990). HP MRS allows for a >10,000-fold increase in sensitivity to detect metabolic tracers labelled with the non-radioactive isotope, carbon-13 [1-^{13}C], enabling in vivo real-

[1]National Heart Research Institute Singapore, National Heart Centre Singapore, Singapore. [2]Cardiovascular and Metabolic Disorders Programme, Duke-NUS Medical School, Singapore. [3]Yong Loo Lin School of Medicine, National University of Singapore, Singapore. [4]The Hatter Cardiovascular Institute, University College London, London, UK. [5]Cardiovascular Research Center, College of Medical and Health Sciences, Asia University, Taiwan.

*Both authors contributed equally

Correspondence should be addressed to Prof Derek J. Hausenloy (derek.hausenloy@duke-nus.edu.sg).

time assessment of substrate uptake and tracking of downstream metabolites (Wang et al., 2019). The most widely used tracer is hyperpolarized [1-^{13}C] pyruvate, which provides information on oxidative metabolism (via hyperpolarized [1-^{13}C] bicarbonate), glycolysis (via hyperpolarized [1-^{13}C] lactate), and amino acid metabolism (via hyperpolarized [1-^{13}C] alanine).

A number of clinical studies have used ^{13}C HP MRS to assess metabolic flux in patients. In 2010, [1-^{13}C] pyruvate was administered to prostate cancer patients to obtain real-time metabolic images of the prostate (University of California and Healthcare, 2010), after which other clinical trials have been initiated to assess patients with various types of cancers, with prostate and neurological neoplasms being the most studied (Chang et al., 2015; Centre, 2016b; University of California et al., 2016; Centre, 2017). ^{13}C HP MRS has also been applied to monitor metabolic events in fatty liver disease and traumatic brain injury (Center, 2018b, c). The use of ^{13}C HP MRS in cardiovascular disease is minimal, but could gain further support pending findings from two on-going clinical trials that are evaluating its application for congestive heart failure and hypertrophic cardiomyopathy (Centre, 2016a; Center, 2018a). Though ^{13}C HP MRS is yet to gain wide-spread clinical implementation, several pre-clinical (Golman et al., 2008; Merritt et al., 2008; Aquaro et al., 2013; Ball et al., 2013; Lau et al., 2013; Dodd et al., 2014; Yoshihara et al., 2015; Oh-Ici et al., 2016) and initial clinical studies (Rider et al., 2020; Apps et al., 2021) have supported the use of hyperpolarized [1-^{13}C] pyruvate-MRS to gain insights into cardiometabolic changes underpinning AMI and diabetic cardiomyopathy. Here, we provide an overview on the use of 13C HP MRS in preclinical and clinical studies, and discuss the feasibility of this innovative strategy to gain unprecedented insight into maladaptive metabolic remodeling that occurs during HF, which may help in the identification of novel metabolic treatment targets for improving health outcomes in patients with cardiac disease.

Metabolic Probes in Cardiac ^{13}C HP MRS

Probes for Energy Production

Unlike PET, which measures myocardium metabolism by imaging the uptake of radioactive glucose or other probes, ^{13}C HP MRS traces the production and consumption of different metabolites simultaneously, yielding information about enzymatic metabolic flux (Schelbert, 1994). Early applications of ^{13}C HP MRS used [1-^{13}C] pyruvate as the probe to examine metabolic flux through the pyruvate dehydrogenase complex (PDH) in animal hearts subjected to ischemic episodes (Golman et al., 2008; Merritt et al., 2008; Schroeder et al., 2008). PDH converts pyruvate into carbon dioxide and acetyl-Coenzyme A (acetyl-CoA), which enters the tricarboxylic acid (TCA) cycle to reduce electron carriers, nicotinamide adenine dinucleotide (NAD) and flavin adenine dinucleotide (FAD), into NADH and $FADH_2$ (Figure 1) (Nelson et al., 2008). Reduced electron carriers transfer high-energy electrons to the electron transport chain, consuming oxygen as final electron acceptors and generating ATP. However, when the cellular oxygen supply is compromised, the electron transport chain is impaired, leading to an accumulation of NADH and $FADH_2$ with concurrent shortage of NAD and FAD (Nelson et al., 2008). Increased NADH/NAD causes the inhibition of PDH, shunting the pyruvate flux away from downstream catabolic reactions and towards lactate production. To restore the intracellular NAD stock, lactate dehydrogenase regenerates NAD from NADH by reducing pyruvate into lactate (Figure 1). In cardiomyocytes, PDH converts [1-^{13}C] pyruvate into acetyl-CoA and $^{13}CO_2$, which becomes ^{13}C-bicarbonate rapidly, while lactate dehydrogenase (LDH) reduces [1-^{13}C] pyruvate into [1-^{13}C] lactate (Figure 1) (Schroeder et al., 2008). Therefore, the measurements of $^{13}CO_2$ /^{13}C-bicarbonate and [1-^{13}C] lactate could potentially identify ischemic myocardium. Moreover, since the conversion between lactate and pyruvate by LDH is reversible, some studies have used [1-^{13}C] lactate as a metabolic probe (Mayer et al., 2012; Lau et al., 2021). Interestingly, alanine transaminase (ALT) could convert cytosolic [1-^{13}C] pyruvate into [1-^{13}C] alanine, which can also be resolved by ^{13}C HP MRS (Figure 1) (Golman et al., 2008; Merritt et al., 2008; Dodd et al., 2012; Menichetti et al., 2012; Dodd et al., 2013; Apps et al., 2018).

During the PDH conversion, the first carbon of pyruvate is converted into CO_2, while the second and third carbon nuclei are converted into acetyl-CoA. Hence, labeling the second carbon of pyruvate with ^{13}C ([2-^{13}C] pyruvate) allows for measuring TCA cycle flux (besides PDH flux) by tracking TCA cycle intermediates and their derivatives, such as [1-^{13}C] citrate and [5-^{13}C] glutamate (Schroeder et al., 2009) (Figure 1). Moreover, the measurement of [1-^{13}C] acetyl-CoA after [2-^{13}C] pyruvate administration provides information on the relative contributions from glucose and fatty acid oxidation for the energy need of cardiomyocytes. Healthy cardiomyocytes fuel their acetyl-CoA pool primarily via β-oxidation of long-chain fatty acids, while glycolysis is activated only under certain circumstances, such as adrenergic stress, ischemia, or late-stage heart failure (Collins-Nakai et al., 1994; Cross et al., 1996; Stanley et al., 2005). As such, ^{13}C HP MRS measurement of glucose contribution to the overall cardiomyocyte acetyl-CoA pool may provide insights into these underlying pathologies.

Besides pyruvate, other metabolic probes have also been developed to monitor the metabolic alterations in cardiomyocytes. For instance, acetate, unlike pyruvate is an acetyl-CoA source independent of PDH, and [1-^{13}C] acetate can be readily converted to acetyl-CoA in the cytosol via acetyl-CoA synthetase (ACS), allowing the possibility to directly monitor TCA flux without being influenced by PDH activity (Bastiaansen et al., 2015; Flori et al., 2015; Koellisch et al., 2015) (Figure 1). Moreover, [1-^{13}C] acetate and [1-^{13}C] acetylcarnitine (the metabolite from cytosolic [1-^{13}C] acetate) have been identified as markers of fatty acid oxidation in the normoxic state (Jensen et al., 2009). Instead of indirectly probing lipid oxidation in cardiomyocytes, medium-chain fatty acids, like [1-^{13}C] octanoate, could also be directly labeled to monitor myocardial fatty acid usage (Yoshihara et al., 2020). Finally, administration of [3-^{13}C] acetoacetate and [1-^{13}C] butyrate allows researchers to monitor the cardiomyocyte metabolic shift to ketone oxidation as a result of changes in diet, diseases, or medications, since both substrates convert to a type of ketone body, [1-^{13}C] β-hydroxybutyrate (β-OHB) (Bastiaansen et al., 2016; Abdurrachim et al., 2019a; Abdurrachim et al., 2019b).

Probes for pH and Redox Potential

^{13}C HP MRS also allows visualization of alterations in local pH and redox state. By monitoring the relative concentration of bicarbonate and CO_2, the pH of the local environment can be calculated using the Henderson-Hasselbalch equation ($pH=pKa+logHCO_3^-/CO_2$, where pKa is ~6.17 (Bogh et al., 2020). Since [1-^{13}C] pyruvate can be converted to $^{13}CO_2$, it has been used to monitor changes in cardiac pH (Merritt et al., 2008; Schroeder et al., 2010; Lau et al., 2017a; Bogh et al., 2020; Bøgh et al., 2020; Chen et al., 2020), and alternatively, ^{13}C-labeled bicarbonate has also been used as a probe to measure local pH in hearts and tumors (Gallagher et al., 2008; Gallagher et al., 2015; Scholz et al., 2015; Korenchan et al., 2016; Korenchan et al., 2019a; Korenchan et al., 2019b).

The redox states of NADP/NADPH and NAD/NADH are associated with the generation of reactive oxygen species (ROS), the latter reported to play critical roles in aging, tumorigenesis, AMI, and HF. NADPH is a reductant involving multiple biosynthetic pathways (e.g., pentose phosphate pathway)

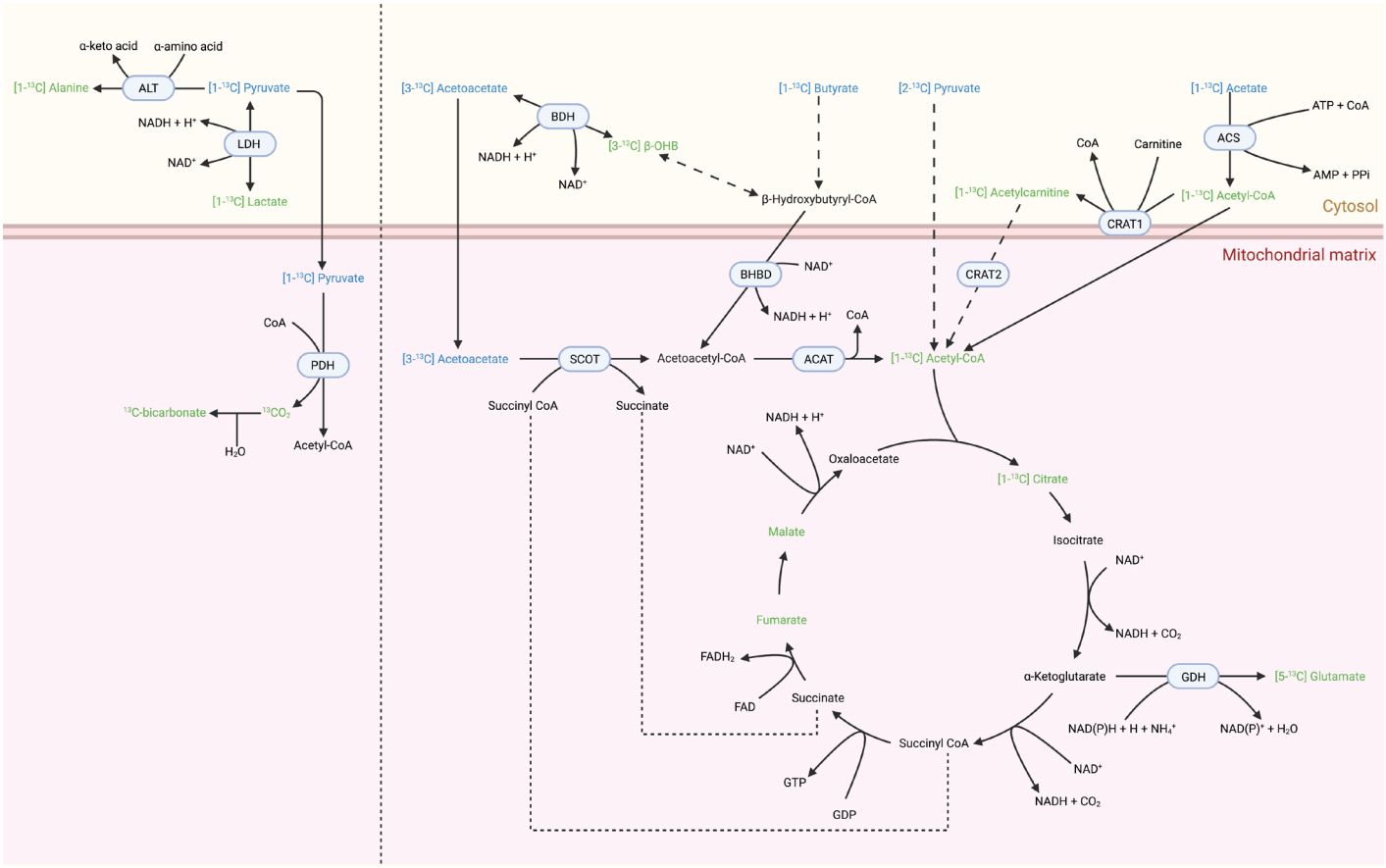

Figure 1. ^{13}C HP MRS probes and downstream metabolites used to track myocardial metabolic changes. Blue: probes administered to subjects. Green: downstream metabolites that can be resolved with ^{13}C HP MRI. ALT: alanine aminotransferase, LDH: lactate dehydrogenase, PDH: pyruvate dehydrogenase, BDH: β-hydroxybutyrate dehydrogenase, SCOT: succinyl-CoA:3-ketoacid CoA transferase (Hasegawa et al., 2012), BHBD: 3-hydroxybutyryl-CoA dehydrogenase (Madan et al., 1973), ACAT: acetyl-CoA acetyltransferase (Goudarzi, 2019), GDH: glutamate dehydrogenase, ACS: acetyl-CoA synthetase, CRAT: carnitine O-acetyltransferase (Bonnefont et al., 2004). Figure was created with BioRender.com

during which NADP is reduced to NADPH. The oxidation of NADPH back to NADP is coupled with the reduction of oxidized glutathione (GSSG) to glutathione (GSH), while oxidation of GSH to GSSG is coupled with the reduction of dehydroascorbate (DHA) to vitamin C (Del Bello et al., 1994; Maellaro et al., 1994; Whitbread et al., 2005; Linster and Van Schaftingen, 2007). Consistently, [1-^{13}C] DHA was rapidly converted to [1-^{13}C] vitamin C in the liver, kidneys, brain, and prostate cancer tumors in mice (Keshari et al., 2011). NADH donates two of its electrons to complex I in the electron transport chain and is oxidized to NAD. Since most of the mitochondrial NADH is protein-bound, direct measurement of free NAD/NADH ratio does not accurately reflect tissue redox state. To overcome this limitation, metabolic flux through LDH and β-hydroxybutyrate dehydrogenase (BDH), which converts acetoacetate to β-hydroxybutyrate (β-OHB) are commonly used as surrogate markers for NAD/NADH redox monitoring (Veech et al., 1969; Veech et al., 1972; Sato et al., 1995; Blinova et al., 2005; Veech, 2006). Finally, by using [1,3-^{13}C] acetoacetate and by monitoring its conversion to [1,3-^{13}C] β-OHB to assess mitochondrial NAD/NADH redox state, Chen et al. (2019) observed an elevation in [1,3-^{13}C] β-OHB in ischemic rat hearts and in hearts inhibited for complex I. These findings supported an accumulation of NADH, which was confirmed by additional enzyme assays (Chen et al., 2019).

Probes for Myocardial Perfusion

Apart from assessing metabolism, ^{13}C HP MRS can also be used to image myocardial perfusion with ^{13}C-urea, the latter being ideal for quantitative perfusion mapping as its HP signals are linearly correlated with its concentration (Wang et al., 2019). In support, ^{13}C-urea HP signals were found to be increased by two-fold during adenosine-induced hyperemia, which was consistent with rodent myocardial perfusion reserve (Lau et al., 2016). Moreover, by co-administering ^{13}C-urea and [1-^{13}C] pyruvate, researchers could simultaneously assess cardiac metabolism and perfusion status, offering a more straightforward way of studying the metabolism/perfusion mismatch (Lau et al., 2017b).

Ischemic Heart Disease

[1-^{13}C] Pyruvate HP MRS Images Metabolic Changes during AMI

In the area of ischemic heart disease, PDH is a well-studied metabolic probe as [1-^{13}C] pyruvate flux through PDH is expected to decrease in ischemic cardiomyocytes. Following induction of ischemia in pig hearts with a balloon catheter, Golman et al. (2008) found that administration of [1-^{13}C] pyruvate resulted in reduced ^{13}C-bicarbonate levels in the affected region after 15 minute occlusion and almost completely diminished after 45-minutes occlusion, during which the affected myocardium underwent infarction. Despite

demonstrating the alteration of ^{13}C-bicarbonate during the ischemia and infarction, the authors were unable to ascertain the change in [1-^{13}C] lactate levels due to presence of artifacts. In the same year, Merritt et al. (2008) demonstrated that while [1-^{13}C] alanine and [1-^{13}C] lactate signals were still detectable after 10 minutes of global ischemia in isolated rat hearts, the $^{13}CO_2$ signal was not detectable during the first 90 seconds of reperfusion. Interestingly, the $^{13}CO_2$ signal was detected at the 20-minute reperfusion time point, suggesting that PDH flux was almost completely ablated during the first 90 seconds of reperfusion and recovered within 20 minutes in non-infarcted myocardium (Merritt et al., 2008).

With the development of imaging technology, PDH flux tracing has acquired increased spatiotemporal resolution. In 2013, Aquaro et al. (2013) employed a fast three-dimensional pulse sequence (3D-IDEAL spiral CSI pulse sequence) to determine the distribution of transient metabolic changes in pig hearts, where the authors successfully identified differential distribution of lactate and bicarbonate signals among ischemic and remote regions in the left ventricle. However, here the authors did not provide actual MR images showing lactate/bicarbonate signal distribution across the ischemic pig heart, but merely summarized the lactate and bicarbonate signal levels in various myocardium segments (Aquaro et al., 2013). When imaging the alterations of metabolites in acute and chronic infarct regions of isolated rat hearts, researchers observed increased lactate signals, but decreased bicarbonate signals in the acute infarct region. Interestingly, in the chronic infarct region, both lactate and bicarbonate signals were found to be diminished (Ball et al., 2013). In other studies, when using 3D-IDEAL spiral CSI pulse sequence in pig hearts, both [1-^{13}C] lactate and ^{13}C-bicarbonate signals were found to be decreased in the affected region during ischemia, and while [1-^{13}C] lactate signals increased during reperfusion, ^{13}C-bicarbonate signals diminished further. Although tracing metabolism changes with HP MRS is more challenging in small animals (e.g., rats), in 2015, Yoshihara et al. (2015) and Oh-Ichi et al. (2016) first developed schemes to track PDH flux with [1-^{13}C] pyruvate in intact rats, and in 2017, Lauritzen et al. (2017) was able to image the in vivo metabolic changes during rat MI in an open-chest model, where the authors found reduced [1-^{13}C] alanine and [1-^{13}C] lactate signals in the infarct region during ischemia. One of the main concerns that need to be addressed when using ^{13}C HP MRS in the clinical setting is its reproducibility and low variability of acquired measurements. In this regard, by normalizing the ^{13}C signal with left ventricular maximum pyruvate signal, Lau et al. (2013) demonstrated the robustness of the application in free-breathing pigs.

Though ^{13}C HP MRS is yet to be adopted as a standard clinical imaging modality, Apps et al. (2021) recently published a case report with two AMI patients undergoing [1-^{13}C] pyruvate HP MRS imaging. In this study, both patients' nonviable transmural infarction region showed an absence of both [1-^{13}C] lactate and ^{13}C-bicarbonate signals, which was otherwise present in the viable subendocardial infarct regions (Apps et al., 2021). This study supports the feasibility of using ^{13}C HP MRS in patients with recent AMI to gain insight into in vivo metabolic flux, for elucidating myocardial response to acute IRI and to help identify novel metabolic targets for preventing post-infarct adverse LV remodeling and HF.

[1-^{13}C] Pyruvate HP MRS as a Secondary Indication of Post-MI Injury and Recovery

Besides monitoring transient PDH flux alteration during ischemia and reperfusion, researchers have also found that [1-^{13}C] pyruvate can be used to monitor local inflammatory responses and necrosis, and can help predict post-MI left ventricular remodeling. In activated monocytes and macrophages, metabolic reprogramming drives these cells to adopt glycolysis as their primary energy-generating pathway due to oxygen efficiency, resulting in an increase in lactate production. In support, Lewis et al. (2018) demonstrated intense [1-^{13}C] lactate signals in the infarct region by day 7 post-MI in rodents and pigs. The authors also found that in the in vitro macrophage suspension, activation and polarization with lipopolysaccharide could augment the [1-^{13}C] lactate signal after [1-^{13}C] pyruvate administration. While blockade of glycolysis with 2-deoxyglucose could normalize the [1-^{13}C] lactate signal in both macrophage suspension and in vivo infarction model, it also resulted in increased expression of interleukin (IL)-1β and improved systolic function in the latter. These findings suggest that the elevation in [1-^{13}C] lactate signals during healing post-MI could indicate monocyte/macrophage reprogramming, which links to their inflammatory function (Lewis et al., 2018). In other studies, researchers demonstrated that ratios among [1-^{13}C] lactate, ^{13}C-bicarbonate, and total carbon correlated with necrosis and local pH changes in early AMI and reperfusion, as necrotic tissues were found to have significantly higher [1-^{13}C] lactate/^{13}C-bicarbonate and [1-^{13}C] lactate/total carbon signal ratios, which negatively correlated with the local pH (Moon et al., 2019). Besides these short-term effects, a low ^{13}C-bicarbonate + $^{13}CO_2$/[1-^{13}C] pyruvate signal ratio has been found to correlate with a reduced left ventricular ejection fraction (LVEF) 3 days post-MI. Interestingly, at 30 days post-MI, a higher ^{13}C-bicarbonate + $^{13}CO_2$/[1-^{13}C] pyruvate signal ratio correlated with poorer recovery of LVEF among rodents that underwent active β-blocker and ACE-inhibitor treatment. These findings suggest that responders to HF medication may have reduced capacity for carbohydrate metabolism (Tougaard et al., 2021).

Application of Non-[1-^{13}C] Pyruvate HP MRS in Ischemic Heart Disease

Besides [1-^{13}C] pyruvate, other metabolic probes have also been applied to study metabolic or pathological alterations in ischemic heart disease. For instance, [2-^{13}C] pyruvate has allowed researchers to track metabolic flux through the TCA cycle as evidenced by Schroeder et al. (2009) who demonstrated that during ischemia, [1-^{13}C] citrate and [5-^{13}C] glutamate signals were reduced, implicating a decreased TCA cycle flux in isolated rat hearts. Moreover, a reduction in PDH flux and TCA cycle flux at 22 weeks post-MI was found to correlate with decreased cardiac function in rats, suggesting an association between alterations in myocardial energy demands and cardiac function (Dodd et al., 2014). In other studies, by using [1-^{13}C] acetate and [1,3-$^{13}C_2$] acetoacetate, researchers observed a decreased reliance of fatty acid oxidation in ischemic heart tissue and NADH accumulation in the mitochondria (Jensen et al., 2009; Chen et al., 2019). Interestingly, in normal cells, [1,4-$^{13}C_2$] fumarate is unable to undergo direct conversion into [1,4-$^{13}C_2$] malate, a reaction which only occurs in necrotic cells with diminished membrane integrity (Gallagher et al., 2009). Taking advantage of this property, Miller et al. (2018) observed an increased [1,4-$^{13}C_2$] malate signal in the necrotic region of rat hearts 1- and 7-days post-MI, with no detection in control rats, thereby supporting the use of specific probes for discriminating between healthy and necrotic cardiac tissue.

Chronic Cardiac Diseases

Metabolic Profile Alteration in Cardiomyopathy Progression

In HF, glucose intake and glycolysis rates increase significantly to compensate for fatty acid oxidation (Karwi et al., 2018). However, these maladaptive metabolic alterations are compounded in the setting of diabetes (Sowton et al., 2019). Insulin resistance can lead to reduced glucose oxidation, but paradoxically increases fatty acid dependency and activates

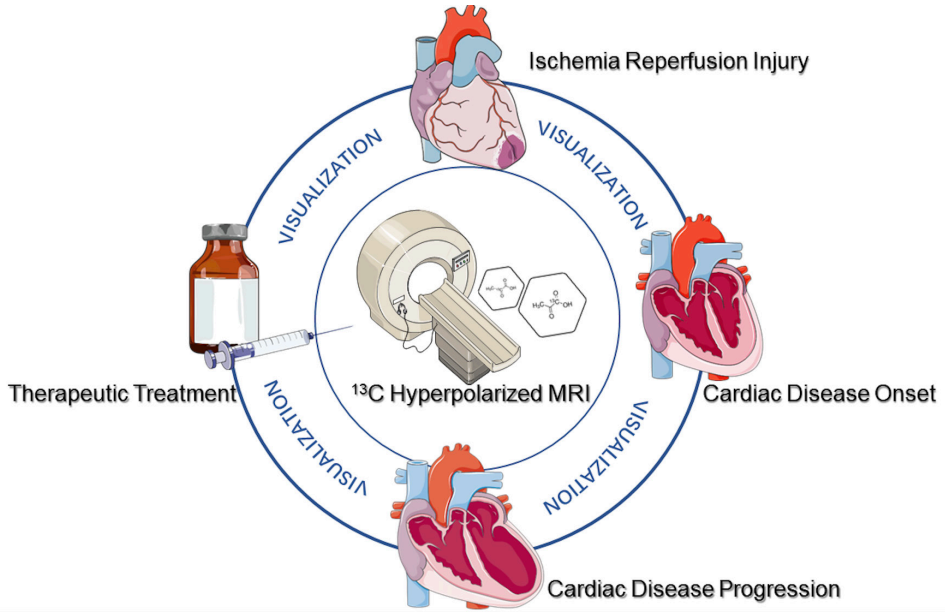

Figure 2. Schematic of the potential clinical application of ^{13}C hyperpolarized magnetic resonance spectroscopy.

β-oxidation (Chong et al., 2017; Cong et al., 2020), and hence, the conversion of metabolic substrates from fatty acids to glucose that occur during HF still remains controversial (He et al., 2021). This, may in part, reflect the heterogeneity of clinical HF syndromes (Lewis et al., 2020) and the demands for techniques that are capable of assessing cardiac energy metabolism during the longitudinal progression of HF (Peterson and Gropler, 2020), and for monitoring the response to metabolism-based therapies (Selvaraj et al., 2020).

^{13}C HP MRS Application in Evaluating the Stage of Cardiomyopathy

The sensitivity and specificity of ^{13}C HP MRS in evaluating cardiomyopathy has long been proven in various animal models. In 2013, Schroeder et al. (2013) reported the successful application of HP ^{13}C MRS in a dilated cardiomyopathy pig model, where administration of [2-^{13}C] pyruvate and [1-^{13}C] pyruvate was able to implicate reduced pyruvate oxidation and impaired Krebs cycle function. Researchers have also tested the feasibility of using metabolic imaging provided by HP MRS as an early indication of impending HF (Agger et al., 2020). In a porcine model of right ventricular heart failure, a significant decrease in the conversion ratio of pyruvate/bicarbonate along with an increase in the lactate/bicarbonate ratio was observed, which together represents a shift towards anaerobic metabolism. Importantly, this phenomenon was observed during the early stage of right ventricular dysfunction as no changes were seen on echocardiography. Similar findings have also been observed in a rodent model of diabetic cardiomyopathy, with a reduction in PDH flux being associated with impaired diastolic function (Le Page et al., 2015). Finally, HP MRS has also been used in systemic metabolic disorders that predominantly manifest in heart tissue as evidenced by a reduction in in vivo pyruvate dehydrogenase flux that correlated with increased cardiac hypertrophy in an animal model of hyperthyroidism (Atherton et al., 2011a).

Although HP pyruvate probes can be used to track carbohydrate metabolism in the heart, they are not suited for directly assessing fatty acid pathways (the preferential substrate of the adult heart) (Ramachandra et al., 2018), nor ketone metabolism, the latter reported to have a critical role in heart failure progression (Voros et al., 2018). Unlike ketone bodies (acetoacetate), long-chain fatty acids require albumin for their solubilization in water, as such, only water-soluble fatty acid intermediates like butyrate and acetate have been employed as probes for HP studies (Ball et al., 2014; Comment and Merritt, 2014) (Figure 1). Recently, Abdurrachim et al. (2019a) revealed increased ketone body utilization in the diabetic heart as evidenced by elevated production of [5-^{13}C] glutamate, which correlated with cardiac hypertrophy and dysfunction. In a follow-up study (Abdurrachim et al., 2019b), the authors injected HP [3-^{13}C] acetoacetate, [1-^{13}C] butyrate, or [1-^{13}C] pyruvate to assess changes in ketone body, short-chain fatty acid, or glucose utilization respectively, in the diabetic heart following long-term low-carbohydrate low-protein ketogenic diet.

Despite the abundant research that has been conducted on animals, the clinical application of ^{13}C HP MRS in HF is still at its infancy. In 2016, following administration of HP [1-^{13}C] pyruvate, Cunningham et al. (2016) introduced the first ^{13}C images of healthy human hearts and successfully detected ^{13}C-bicarbonate signals, highlighting the feasibility of assessing pyruvate metabolism in humans. More recently, the first human case-control study to investigate cardiac metabolism changes in type 2 diabetes and healthy hearts using HP [1-^{13}C] pyruvate has been conducted (Rider et al., 2020). In this study, by assessing the downstream metabolism of [1-^{13}C] pyruvate (Figure 1) ([^{13}C] bicarbonate, [1-^{13}C] lactate, and [1-^{13}C] alanine), metabolic flux through cardiac pyruvate dehydrogenase was found to be significantly reduced in type 2 diabetes mellitis patients, demonstrating the feasibility of this non-invasive imaging modality to detect metabolic disturbances in patients with diabetic cardiomyopathy.

^{13}C HP MRS Application and therapeutic targeting of metabolism

In addition to evaluating the metabolic changes that occur in cardiac disease, ^{13}C HP MRS has also been used to assess the effects of pharmacological intervention that target metabolic pathways in the heart, allowing for validation of new treatment targets and strategies for preventing cardiac disease (Hesketh and Brindle, 2018; Wang et al., 2019).

In this regard, given that PDH appears to play a central role in balancing substrate utilization, its modulation could be a considered as a promising therapeutic strategy for HF (Mayers et al., 2005; Timm et al., 2018). In support, treatment with dichloroacetate (DCA), a classical pyruvate dehydrogenase kinase (PDK) inhibitor, was found to restore PDH flux

to normal levels in diabetic hearts, which in turn, led to rebalancing of myocardial substrate selection with subsequent improvements in diastolic function (Le Page et al., 2015). These findings were validated in a porcine right ventricular HF model (Bøgh et al., 2020), where oral administration of DCA augmented carbohydrate metabolism, which directly improved the contractile reserve of the heart. In a mouse diabetic cardiomyopathy model, imaging with HP [1-^{13}C] pyruvate showed PS10 (a more selective PDK inhibitor) stimulated PDC flux, without activating the anaerobic glycolysis pathway, whereas DCA was shown to activate both pathways, positioning PS10 treatment to be more suitable for diabetic cardiomyopathy (Wu et al., 2018). Finally, HP MRS has shown L-carnitine to alleviate myocardial dysfunction by augmenting PDH flux post-ischemia in type 1 diabetic rats (Savic et al., 2021).

Apart from evaluating maladaptive metabolism and functional effects of novel therapeutic compounds, ^{13}C HP MRS has also been used to investigate the mechanisms underlying the unexpected cardiovascular effects of metabolism-targeting drugs. For instance, HP [1-^{13}C] pyruvate MRS has been used to demonstrate previously unrecognized effects of metformin on cardiac redox state (Lewis et al., 2016). Similarly, researchers have attempted to elucidate the mode of action of empagliflozin, a sodium-glucose co-transporter-2 inhibitor (SGLT2i) that has been shown to reduce cardiac afterload in a hypertensive HF rat model (Abdurrachim et al., 2019a). In this study, using a novel ketone probe (HP [3-^{13}C] acetoacetate), the authors found the beneficial effects of SGLT2i treatment on heart function were not associated with any changes in myocardial glucose and ketone utilization (Abdurrachim et al., 2019a). These findings are particularly interesting and topical given the recent report that treatment with SGLT2i therapy improved clinical outcomes in patients with heart failure with preserved ejection fraction (HFpEF) (Anker et al., 2021), another condition characterized by diastolic dysfunction – crucially, the mechanisms underlying the beneficial cardiovascular effects of this class of drugs remain unclear. Therefore, HP MRS may provide novel metabolic insights into the pathophysiology of HFpEF and help elucidate the mechanisms through which SGLT2i therapy prevents heart failure hospitalization.

Limitations and Challenges with HP MRS

Although HP MRS has shown initial promise in patients with cardiac disease (see Figure 2), there are some challenges and limitations to this approach. The potential of extending the diagnostic value of HP MRS from ischemic heart disease towards chronic heart failure (e.g., diabetic cardiomyopathy) has raised some concerns about the applicability of the most widely used first-order kinetics model in previous HP pyruvate studies (Mariotti et al., 2016; Chen et al., 2018). Data have shown that the measurement of metabolism of isolated hearts is highly susceptible towards the effects of competing substrates and pyruvate product inhibition (Moreno et al., 2010; Mariotti et al., 2016). Thus, during the in vitro HP MRS procedure, after the infusion of supra-physiological concentrations of pyruvate (3.3 mM in heart), the PDH flux might not follow first-order kinetics but undergo transient perturbation relating to exhaustion of cofactors like NAD^+, which requires a non-linear model to fit if comparison of quantification is needed (Mariotti et al., 2016). Additionally, because of the evident feedback inhibition of pyruvate over the glycolysis process, it is advised HP pyruvate not be used to measure the glycolysis variation, a typical change during the progression of heart failure (Williamson and Jones, 1964; Neubauer, 2007). However, compared to ex-vivo measurements, preclinical and clinical studies have only adopted 0.1-140mol/kg dose of HP pyruvate injection (Cunningham et al., 2016; Rider et al., 2020), which results in maximum plasma concentrations of ~250 μM of pyruvate, (equivalent to its physiological concentration), and these studies have shown minimal variation of other metabolites during the pyruvate infusion (Atherton et al., 2011b). As such, further investigations are needed to justify the use of HP MRS and optimize the dose of HP compounds before clinical application, and the obtained metabolic data should be interpreted with caution.

One major limitation of HP MRS relates to the molecules used in imaging, in terms of their physicochemical properties (e.g., short T1 relaxation time), and biological properties (e.g., fast cellular uptake and metabolism) (Sowton et al., 2019; Apps et al., 2018). The effect of this is that only a few metabolites can be used as hyperpolarized tracers (Miloushev et al., 2016), thereby restricting metabolic assessment to glucose, lipid, and amino acid metabolism (Apps et al., 2018). Moreover, another drawback that impedes the bench-to-bedside translation of HP MRS is the very rapid decay (~20-30s in vivo) of the polarization of the ^{13}C probes following dissolution (Brindle, 2015), which prohibits the HP MRS techniques from being used to study gradual metabolic reactions. Moreover, due to this short time window, the hyperpolarization facilities (only available in very few centers worldwide) need to be kept within a very short distance from MR scanners to minimize losses in ^{13}C polarization, implying that this innovative technology could not be widely accessible under the current situation (Comment and Merritt, 2014; Lewis et al., 2020). Another technical concern regarding HP MRS is its relatively poor spatial resolution, which may be solved by optimizing the signal-to-noise ratio or by combining PET/CT to provide more information on substrate uptake (Ntziachristos et al., 2019). Regardless of these challenges, HP MRS has tremendous potential for gaining novel metabolic insights into a number of diverse cardiac diseases characterized by metabolic perturbations.

Conclusion

Metabolic perturbations are known to contribute to the pathophysiology of a variety of cardiac diseases including AMI, HFpEF, hypertrophic cardiomyopathy, dilated cardiomyopathy, post-partum cardiomyopathy, and diabetic cardiomyopathy. The emergence of ^{13}C HP MRS has provided the unique opportunity to assess metabolic flux in the healthy and diseased heart. Although the majority of data have been confined to pre-clinical animal studies, the feasibility of undertaking HP MRS in patients with cardiac disease has recently been demonstrated in the setting of AMI and diabetic cardiomyopathy. Therefore, HP MS offers the potential to evaluate the metabolic disturbances underlying a number of cardiac diseases and should result in the identification of novel metabolic treatment targets and strategies for improving outcomes in patients with HF.

Conflict of Interest:

The authors declare they have no conflict of interests.

Acknowledgement

Derek Hausenloy is Duke-National University Singapore Medical School, Singapore Ministry of Health's National Medical Research Council under its Clinician Scientist-Senior Investigator scheme (NMRC/CSA-SI/0011/2017) and Collaborative Centre Grant scheme (NMRC/CGAug16C006). This article is based upon work from COST Action EU-CARDIOPROTECTION CA16225 supported by COST (European Cooperation in Science and Technology). Chrishan Ramachandra is supported by the Singapore Ministry of Health's National Medical Research Council under its Open Fund-Young Individual Research Grant (NMRC/OFYIRG/0073/2018) and the SingHealth Duke-NUS Academic Medical Centre under its SingHealth Duke-NUS Academic Medicine Research Grant (AM/TP033/2020 [SRDUKAMR2033]).

References

Abdurrachim D, Teo XQ, Woo CC, Chan WX, Lalic J, Lam CSP, Lee PTH (2019a) Empagliflozin reduces myocardial ketone utilization while preserving glucose utilization in diabetic hypertensive heart disease: A hyperpolarized (13) C magnetic resonance spectroscopy study. Diabetes Obes Metab 21:357-365.

Abdurrachim D, Teo XQ, Woo CC, Ong SY, Salleh NF, Lalic J, Tan RS, Lee PTH (2019b) Cardiac metabolic modulation upon low-carbohydrate low-protein ketogenic diet in diabetic rats studied in vivo using hyperpolarized (13) C pyruvate, butyrate and acetoacetate probes. Diabetes Obes Metab 21:949-960.

Agger P, Hyldebrandt JA, Hansen ESS, Omann C, Bogh N, Waziri F, Nielsen PM, Laustsen C (2020) Magnetic resonance hyperpolarization imaging detects early myocardial dysfunction in a porcine model of right ventricular heart failure. Eur Heart J Cardiovasc Imaging 21:93-101.

Anker SD et al. (2021) Empagliflozin in Heart Failure with a Preserved Ejection Fraction. N Engl J Med.

Apps A, Lau J, Peterzan M, Neubauer S, Tyler D, Rider O (2018) Hyperpolarised magnetic resonance for in vivo real-time metabolic imaging. Heart 104:1484-1491.

Apps A, Lau JYC, Miller J, Tyler A, Young LAJ, Lewis AJM, Barnes G, Trumper C, Neubauer S, Rider OJ, Tyler DJ (2021) Proof-of-Principle Demonstration of Direct Metabolic Imaging Following Myocardial Infarction Using Hyperpolarized ^{13}C CMR. JACC Cardiovasc Imaging 14:1285-1288.

Aquaro GD, Frijia F, Positano V, Menichetti L, Santarelli MF, Ardenkjaer-Larsen JH, Wiesinger F, Lionetti V, Romano SL, Bianchi G, Neglia D, Giovannetti G, Schulte RF, Recchia FA, Landini L, Lombardi M (2013) 3D CMR mapping of metabolism by hyperpolarized ^{13}C-pyruvate in ischemia-reperfusion. JACC Cardiovasc Imaging 6:743-744.

Ardenkjaer-Larsen JH, Fridlund B, Gram A, Hansson G, Hansson L, Lerche MH, Servin R, Thaning M, Golman K (2003) Increase in signal-to-noise ratio of > 10,000 times in liquid-state NMR. Proc Natl Acad Sci U S A 100:10158-10163.

Atherton HJ, Dodd MS, Heather LC, Schroeder MA, Griffin JL, Radda GK, Clarke K, Tyler DJ (2011a) Role of pyruvate dehydrogenase inhibition in the development of hypertrophy in the hyperthyroid rat heart: a combined magnetic resonance imaging and hyperpolarized magnetic resonance spectroscopy study. Circulation 123:2552-2561.

Atherton HJ, Schroeder MA, Dodd MS, Heather LC, Carter EE, Cochlin LE, Nagel S, Sibson NR, Radda GK, Clarke K, Tyler DJ (2011b) Validation of the in vivo assessment of pyruvate dehydrogenase activity using hyperpolarised ^{13}C MRS. NMR Biomed 24:201-208.

Ball DR, Cruickshank R, Carr CA, Stuckey DJ, Lee P, Clarke K, Tyler DJ (2013) Metabolic imaging of acute and chronic infarction in the perfused rat heart using hyperpolarised [1-^{13}C]pyruvate. NMR Biomed 26:1441-1450.

Ball DR, Rowlands B, Dodd MS, Le Page L, Ball V, Carr CA, Clarke K, Tyler DJ (2014) Hyperpolarized butyrate: a metabolic probe of short chain fatty acid metabolism in the heart. Magn Reson Med 71:1663-1669.

Bastiaansen JA, Cheng T, Lei H, Gruetter R, Comment A (2015) Direct noninvasive estimation of myocardial tricarboxylic acid cycle flux in vivo using hyperpolarized (1)(3)C magnetic resonance. J Mol Cell Cardiol 87:129-137.

Bastiaansen JAM, Merritt ME, Comment A (2016) Measuring changes in substrate utilization in the myocardium in response to fasting using hyperpolarized [1-^{13}C]butyrate and [1-13C]pyruvate. Scientific Reports 6:25573.

Blinova K, Carroll S, Bose S, Smirnov AV, Harvey JJ, Knutson JR, Balaban RS (2005) Distribution of mitochondrial NADH fluorescence lifetimes: steady-state kinetics of matrix NADH interactions. Biochemistry 44:2585-2594.

Bogh N, Hansen ESS, Mariager CO, Bertelsen LB, Ringgaard S, Laustsen C (2020) Cardiac pH-Imaging With Hyperpolarized MRI. Front Cardiovasc Med 7:603674.

Bøgh N, Hansen ESS, Omann C, Lindhardt J, Nielsen PM, Stephenson RS, Laustsen C, Hjortdal VE, Agger P (2020) Increasing carbohydrate oxidation improves contractile reserves and prevents hypertrophy in porcine right heart failure. Sci Rep 10:8158.

Bonnefont JP, Djouadi F, Prip-Buus C, Gobin S, Munnich A, Bastin J (2004) Carnitine palmitoyltransferases 1 and 2: biochemical, molecular and medical aspects. Mol Aspects Med 25:495-520.

Brindle KM (2015) Imaging metabolism with hyperpolarized (13)C-labeled cell substrates. J Am Chem Soc 137:6418-6427.

Center UoTSM (2018a) UTSW HP 13-C Pyruvate Injection in HCM. In: https://ClinicalTrials.gov/show/NCT03057002.

Center UoTSM (2018b) Imaging of Traumatic Brain Injury Metabolism Using Hyperpolarized Carbon-13 Pyruvate. In: https://ClinicalTrials.gov/show/NCT03502967.

Center UoTSM (2018c) Effect of Fatty Liver on TCA Cycle Flux and the Pentose Phosphate Pathway. In: https://ClinicalTrials.gov/show/NCT03480594.

Centre SHS (2016a) Metabolic Imaging of the Heart Using Hyperpolarized (^{13}C) Pyruvate Injection. In: https://ClinicalTrials.gov/show/NCT02648009.

Centre SHS (2016b) Hyperpolarized Carbon-13 Imaging of Metastatic Prostate Cancer. In: https://ClinicalTrials.gov/show/NCT02844647.

Centre SHS (2017) Study to Evaluate the Feasibility of 13-C Pyruvate Imaging in Breast Cancer Patients Receiving Neoadjuvant Chemotherapy. In: https://ClinicalTrials.gov/show/NCT03121989.

Chang S, Institute NC, University of California SF (2015) Hyperpolarized Imaging in Diagnosing Participants With Glioma. In: https://ClinicalTrials.gov/show/NCT03739411.

Chen AP, Lau AZ, Gu YP, Schroeder MA, Barry J, Cunningham CH (2018) Probing the cardiac malate-aspartate shuttle non-invasively using hyperpolarized [1,2-(13) C2] pyruvate. NMR Biomed 31.

Chen HY, Aggarwal R, Bok RA, Ohliger MA, Zhu Z, Lee P, Gordon JW, van Criekinge M, Carvajal L, Slater JB, Larson PEZ, Small EJ, Kurhanewicz J, Vigneron DB (2020) Hyperpolarized (13)C-pyruvate MRI detects real-time metabolic flux in prostate cancer metastases to bone and liver: a clinical feasibility study. Prostate Cancer Prostatic Dis 23:269-276.

Chen W, Sharma G, Jiang W, Maptue NR, Malloy CR, Sherry AD, Khemtong C (2019) Metabolism of hyperpolarized ^{13}C-acetoacetate to β-hydroxybutyrate detects real-time mitochondrial redox state and dysfunction in heart tissue. NMR in Biomedicine 32:e4091.

Chong CR, Clarke K, Levelt E (2017) Metabolic Remodeling in Diabetic Cardiomyopathy. Cardiovasc Res 113:422-430.

Collins-Nakai RL, Noseworthy D, Lopaschuk GD (1994) Epinephrine increases ATP production in hearts by preferentially increasing glucose metabolism. Am J Physiol 267:H1862-1871.

Comment A, Merritt ME (2014) Hyperpolarized magnetic resonance as a sensitive detector of metabolic function. Biochemistry 53:7333-7357.

Cong S, Ramachandra CJA, Mai Ja KM, Yap J, Shim W, Wei L, Hausenloy DJ (2020) Mechanisms underlying diabetic cardiomyopathy: From pathophysiology to novel therapeutic targets. Cond Med 3:82-97.

Cross HR, Opie LH, Radda GK, Clarke K (1996) Is a high glycogen content beneficial or detrimental to the ischemic rat heart? A controversy resolved. Circ Res 78:482-491.

Cunningham CH, Lau JY, Chen AP, Geraghty BJ, Perks WJ, Roifman I, Wright GA, Connelly KA (2016) Hyperpolarized ^{13}C Metabolic MRI of the Human Heart: Initial Experience. Circ Res 119:1177-1182.

Del Bello B, Maellaro E, Sugherini L, Santucci A, Comporti M, Casini AF (1994) Purification of NADPH-dependent dehydroascorbate reductase from rat liver and its identification with 3 alpha-hydroxysteroid dehydrogenase. Biochem J 304 (Pt 2):385-390.

Dodd MS, Ball V, Bray R, Ashrafian H, Watkins H, Clarke K, Tyler DJ (2013) In vivo mouse cardiac hyperpolarized magnetic resonance spectroscopy. J Cardiovasc Magn Reson 15:19.

Dodd MS, Atherton HJ, Carr CA, Stuckey DJ, West JA, Griffin JL, Radda GK, Clarke K, Heather LC, Tyler DJ (2014) Impaired in vivo mitochondrial Krebs cycle activity after myocardial infarction assessed using hyperpolarized magnetic resonance spectroscopy. Circ Cardiovasc Imaging 7:895-904.

Dodd MS, Ball DR, Schroeder MA, Le Page LM, Atherton HJ, Heather LC, Seymour AM, Ashrafian H, Watkins H, Clarke K, Tyler DJ (2012) In vivo alterations in cardiac metabolism and function in the spontaneously hypertensive rat heart. Cardiovasc Res 95:69-76.

Flori A, Liserani M, Frijia F, Giovannetti G, Lionetti V, Casieri V, Positano V, Aquaro GD, Recchia FA, Santarelli MF, Landini L, Ardenkjaer-Larsen JH, Menichetti L (2015) Real-time cardiac metabolism assessed with hyperpolarized [1-(13) C]acetate in a large-animal model. Contrast Media Mol Imaging 10:194-202.

Gallagher FA, Kettunen MI, Hu D-E, Jensen PR, Karlsson M, Gisselsson A, Nelson SK, Witney TH, Bohndiek SE, Hansson G (2009) Production of hyperpolarized [1, 4-$^{13}C_2$] malate from [1, 4-$^{13}C_2$] fumarate is a marker of cell necrosis and treatment response in tumors. Proceedings of the National Academy of Sciences 106:19801-19806.

Gallagher FA, Kettunen MI, Day SE, Hu DE, Ardenkjaer-Larsen JH, Zandt R, Jensen PR, Karlsson M, Golman K, Lerche MH, Brindle KM (2008) Magnetic resonance imaging of pH in vivo using hyperpolarized ^{13}C-labelled bicarbonate. Nature 453:940-943.

Gallagher FA, Sladen H, Kettunen MI, Serrao EM, Rodrigues TB, Wright A, Gill AB, McGuire S, Booth TC, Boren J, McIntyre A, Miller JL, Lee SH, Honess D, Day SE, Hu DE, Howat WJ, Harris AL, Brindle KM (2015) Carbonic Anhydrase Activity Monitored In Vivo by Hyperpolarized ^{13}C-Magnetic Resonance Spectroscopy Demonstrates Its Importance for pH Regulation in Tumors. Cancer Res 75:4109-4118.

Golman K, Zandt RI, Lerche M, Pehrson R, Ardenkjaer-Larsen JH (2006) Metabolic imaging by hyperpolarized ^{13}C magnetic resonance imaging for in vivo tumor diagnosis. Cancer Res 66:10855-10860.

Golman K, Petersson JS, Magnusson P, Johansson E, Akeson P, Chai CM, Hansson G, Mansson S (2008) Cardiac metabolism measured noninvasively by hyperpolarized ^{13}C MRI. Magn Reson Med 59:1005-1013.

Goudarzi A (2019) The recent insights into the function of ACAT1: A possible anti-cancer therapeutic target. Life Sci 232:116592.

Hasegawa S, Noda K, Maeda A, Matsuoka M, Yamasaki M, Fukui T (2012) Acetoacetyl-CoA synthetase, a ketone body-utilizing enzyme, is controlled by SREBP-2 and affects serum cholesterol levels. Mol Genet Metab 107:553-560.

He Y, Huang W, Zhang C, Chen L, Xu R, Li N, Wang F, Han L, Yang M, Zhang D (2021) Energy metabolism disorders and potential therapeutic drugs in heart failure. Acta Pharm Sin B 11:1098-1116.

Hesketh RL, Brindle KM (2018) Magnetic resonance imaging of cancer metabolism with hyperpolarized (13)C-labeled cell metabolites. Curr Opin Chem Biol 45:187-194.

Jensen PR, Peitersen T, Karlsson M, in 't Zandt R, Gisselsson A, Hansson G, Meier S, Lerche MH (2009) Tissue-specific Short Chain Fatty Acid Metabolism and Slow Metabolic Recovery after Ischemia from Hyperpolarized NMR in Vivo*. Journal of Biological Chemistry 284:36077-36082.

Karwi QG, Uddin GM, Ho KL, Lopaschuk GD (2018) Loss of Metabolic Flexibility in the Failing Heart. Front Cardiovasc Med 5:68.

Keshari KR, Kurhanewicz J, Bok R, Larson PEZ, Vigneron DB, Wilson DM (2011) Hyperpolarized ¹³C dehydroascorbate as an endogenous redox sensor for in vivo metabolic imaging. Proceedings of the National Academy of Sciences 108:18606-18611.

Koellisch U, Gringeri CV, Rancan G, Farell EV, Menzel MI, Haase A, Schwaiger M, Schulte RF (2015) Metabolic imaging of hyperpolarized [1-(13) C]acetate and [1-(13) C]acetylcarnitine - investigation of the influence of dobutamine induced stress. Magn Reson Med 74:1011-1018.

Korenchan DE, Flavell RR, Baligand C, Sriram R, Neumann K, Sukumar S, VanBrocklin H, Vigneron DB, Wilson DM, Kurhanewicz J (2016) Dynamic nuclear polarization of biocompatible (13)C-enriched carbonates for in vivo pH imaging. Chem Commun (Camb) 52:3030-3033.

Korenchan DE, Bok R, Sriram R, Liu K, Santos RD, Qin H, Lobach I, Korn N, Wilson DM, Kurhanewicz J, Flavell RR (2019a) Hyperpolarized in vivo pH imaging reveals grade-dependent acidification in prostate cancer. Oncotarget 10:6096-6110.

Korenchan DE, Gordon JW, Subramaniam S, Sriram R, Baligand C, VanCriekinge M, Bok R, Vigneron DB, Wilson DM, Larson PEZ, Kurhanewicz J, Flavell RR (2019b) Using bidirectional chemical exchange for improved hyperpolarized [(13) C]bicarbonate pH imaging. Magn Reson Med 82:959-972.

Labbe SM, Grenier-Larouche T, Noll C, Phoenix S, Guerin B, Turcotte EE, Carpentier AC (2012) Increased myocardial uptake of dietary fatty acids linked to cardiac dysfunction in glucose-intolerant humans. Diabetes 61:2701-2710.

Lau AZ, Miller JJ, Tyler DJ (2017a) Mapping of intracellular pH in the in vivo rodent heart using hyperpolarized [1-^{13}C] pyruvate. Magn Reson Med 77:1810-1817.

Lau AZ, Chen AP, Cunningham CH (2021) Cardiac metabolic imaging using hyperpolarized [1-$^{(13)}$C]lactate as a substrate. NMR Biomed 34:e4532.

Lau AZ, Miller JJ, Robson MD, Tyler DJ (2016) Cardiac perfusion imaging using hyperpolarized $^{(13)}$C urea using flow sensitizing gradients. Magn Reson Med 75:1474-1483.

Lau AZ, Miller JJ, Robson MD, Tyler DJ (2017b) Simultaneous assessment of cardiac metabolism and perfusion using copolarized [1-$^{(13)}$ C]pyruvate and $^{(13)}$ C-urea. Magn Reson Med 77:151-158.

Lau AZ, Chen AP, Barry J, Graham JJ, Dominguez-Viqueira W, Ghugre NR, Wright GA, Cunningham CH (2013) Reproducibility study for free-breathing measurements of pyruvate metabolism using hyperpolarized $^{(13)}$C in the heart. Magn Reson Med 69:1063-1071.

Lauritzen MH, Magnusson P, Laustsen C, Butt SA, Ardenkjaer-Larsen JH, Sogaard LV, Paulson OB, Akeson P (2017) Imaging Regional Metabolic Changes in the Ischemic Rat Heart In Vivo Using Hyperpolarized [1-$^{(13)}$C]Pyruvate. Tomography 3:123-130.

Le Page LM, Rider OJ, Lewis AJ, Ball V, Clarke K, Johansson E, Carr CA, Heather LC, Tyler DJ (2015) Increasing Pyruvate Dehydrogenase Flux as a Treatment for Diabetic Cardiomyopathy: A Combined ^{13}C Hyperpolarized Magnetic Resonance and Echocardiography Study. Diabetes 64:2735-2743.

Lewis AJ, Miller JJ, McCallum C, Rider OJ, Neubauer S, Heather LC, Tyler DJ (2016) Assessment of Metformin-Induced Changes in Cardiac and Hepatic Redox State Using Hyperpolarized[1-^{13}C]Pyruvate. Diabetes 65:3544-3551.

Lewis AJM, Tyler DJ, Rider O (2020) Clinical Cardiovascular Applications of Hyperpolarized Magnetic Resonance. Cardiovasc Drugs Ther 34:231-240.

Lewis AJM, Miller JJ, Lau AZ, Curtis MK, Rider OJ, Choudhury RP, Neubauer S, Cunningham CH, Carr CA, Tyler DJ (2018) Noninvasive Immunometabolic Cardiac Inflammation Imaging Using Hyperpolarized Magnetic Resonance. Circ Res 122:1084-1093.

Linster CL, Van Schaftingen E (2007) Vitamin C. Biosynthesis, recycling and degradation in mammals. Febs j 274:1-22.

Madan VK, Hillmer P, Gottschalk G (1973) Purification and properties of NADP-dependent L(+)-3-hydroxybutyryl-CoA dehydrogenase from Clostridium kluyveri. Eur J Biochem 32:51-56.

Maellaro E, Del Bello B, Sugherini L, Santucci A, Comporti M, Casini AF (1994) Purification and characterization of glutathione-dependent dehydroascorbate reductase from rat liver. Biochem J 301 (Pt 2):471-476.

Mariotti E, Orton MR, Eerbeek O, Ashruf JF, Zuurbier CJ, Southworth R, Eykyn TR (2016) Modeling non-linear kinetics of hyperpolarized [1-(13)C] pyruvate in the crystalloid-perfused rat heart. NMR Biomed 29:377-386.

Mayer D, Yen YF, Josan S, Park JM, Pfefferbaum A, Hurd RE, Spielman DM (2012) Application of hyperpolarized [1-(1)(3)C]lactate for the in vivo investigation of cardiac metabolism. NMR Biomed 25:1119-1124.

Mayers RM, Leighton B, Kilgour E (2005) PDH kinase inhibitors: a novel therapy for Type II diabetes? Biochem Soc Trans 33:367-370.

Menichetti L, Frijia F, Flori A, Wiesinger F, Lionetti V, Giovannetti G, Aquaro GD, Recchia FA, Ardenkjaer-Larsen JH, Santarelli MF, Lombardi M (2012) Assessment of real-time myocardial uptake and enzymatic conversion of hyperpolarized [1-(1)(3)C]pyruvate in pigs using slice selective magnetic resonance spectroscopy. Contrast Media Mol Imaging 7:85-94.

Merritt ME, Harrison C, Storey C, Sherry AD, Malloy CR (2008) Inhibition of carbohydrate oxidation during the first minute of reperfusion after brief ischemia: NMR detection of hyperpolarized $^{13}CO_2$ and $H^{13}CO_3$. Magn Reson Med 60:1029-1036.

Miller JJ, Lau AZ, Nielsen PM, McMullen-Klein G, Lewis AJ, Jespersen NR, Ball V, Gallagher FA, Carr CA, Laustsen C, Bøtker HE, Tyler DJ, Schroeder MA (2018) Hyperpolarized [1,4-$^{13}C_2$]Fumarate Enables Magnetic Resonance-Based Imaging of Myocardial Necrosis. JACC: Cardiovascular Imaging 11:1594-1606.

Miloushev VZ, Keshari KR, Holodny AI (2016) Hyperpolarization MRI: Preclinical Models and Potential Applications in Neuroradiology. Topics in Magnetic Resonance Imaging 25:31-37.

Moon CM, Kim YH, Ahn YK, Jeong MH, Jeong GW (2019) Metabolic alterations in acute myocardial ischemia-reperfusion injury and necrosis using in vivo hyperpolarized [1-(13)C] pyruvate MR spectroscopy. Sci Rep 9:18427.

Moreno KX, Sabelhaus SM, Merritt ME, Sherry AD, Malloy CR (2010) Competition of pyruvate with physiological substrates for oxidation by the heart: implications for studies with hyperpolarized [1-^{13}C]pyruvate. Am J Physiol Heart Circ Physiol 298:H1556-1564.

Nelson DL, Lehninger AL, Cox MM (2008) Lehninger Principles of Biochemistry: W. H. Freeman.

Neubauer S (2007) The Failing Heart — An Engine Out of Fuel. New England Journal of Medicine 356:1140-1151.

Ntziachristos V, Pleitez MA, Aime S, Brindle KM (2019) Emerging Technologies to Image Tissue Metabolism. Cell Metab 29:518-538.

Oh-Ici D, Wespi P, Busch J, Wissmann L, Krajewski M, Weiss K, Sigfridsson A, Messroghli D, Kozerke S (2016) Hyperpolarized Metabolic MR Imaging of Acute Myocardial Changes and Recovery after Ischemia-Reperfusion in a Small-Animal Model. Radiology 278:742-751.

Peterson LR, Gropler RJ (2020) Metabolic and Molecular Imaging of the Diabetic Cardiomyopathy. Circ Res 126:1628-1645.

Ramachandra CJA, Mai Ja KPM, Lin YH, Shim W, Boisvert WA, Hausenloy DJ (2019) Induced Pluripotent Stem Cells for Modelling Energetic Alterations in Hypertrophic Cardiomyopathy. Cond Med 2:142-151.

Ramachandra CJA, Chua J, Cong S, Kp MMJ, Shim W, Wu JC, Hausenloy DJ (2021) Human-induced pluripotent stem cells for modelling metabolic perturbations and impaired bioenergetics underlying cardiomyopathies. Cardiovasc Res 117:694-711.

Ramachandra CJA, Mehta A, Wong P, Ja K, Fritsche-Danielson R, Bhat RV, Hausenloy DJ, Kovalik JP, Shim W (2018) Fatty acid metabolism driven mitochondrial bioenergetics promotes advanced developmental phenotypes in human induced pluripotent stem cell derived cardiomyocytes. Int J Cardiol 272:288-297.

Rider OJ, Apps A, Miller J, Lau JYC, Lewis AJM, Peterzan MA, Dodd MS, Lau AZ, Trumper C, Gallagher FA, Grist JT, Brindle KM, Neubauer S, Tyler DJ (2020) Noninvasive In Vivo Assessment of Cardiac Metabolism in the Healthy

and Diabetic Human Heart Using Hyperpolarized (13)C MRI. Circ Res 126:725-736.

Sato K, Kashiwaya Y, Keon CA, Tsuchiya N, King MT, Radda GK, Chance B, Clarke K, Veech RL (1995) Insulin, ketone bodies, and mitochondrial energy transduction. Faseb j 9:651-658.

Savic D, Ball V, Curtis MK, Sousa Fialho MDL, Timm KN, Hauton D, West J, Griffin J, Heather LC, Tyler DJ (2021) L-Carnitine Stimulates In Vivo Carbohydrate Metabolism in the Type 1 Diabetic Heart as Demonstrated by Hyperpolarized MRI. Metabolites 11.

Schelbert HR (1994) Metabolic imaging to assess myocardial viability. J Nucl Med 35:8s-14s.

Scholz DJ, Janich MA, Köllisch U, Schulte RF, Ardenkjaer-Larsen JH, Frank A, Haase A, Schwaiger M, Menzel MI (2015) Quantified pH imaging with hyperpolarized (13) C-bicarbonate. Magn Reson Med 73:2274-2282.

Schroeder MA, Cochlin LE, Heather LC, Clarke K, Radda GK, Tyler DJ (2008) In vivo assessment of pyruvate dehydrogenase flux in the heart using hyperpolarized carbon-13 magnetic resonance. Proc Natl Acad Sci U S A 105:12051-12056.

Schroeder MA, Swietach P, Atherton HJ, Gallagher FA, Lee P, Radda GK, Clarke K, Tyler DJ (2010) Measuring intracellular pH in the heart using hyperpolarized carbon dioxide and bicarbonate: a ^{13}C and ^{31}P magnetic resonance spectroscopy study. Cardiovasc Res 86:82-91.

Schroeder MA, Atherton HJ, Ball DR, Cole MA, Heather LC, Griffin JL, Clarke K, Radda GK, Tyler DJ (2009) Real-time assessment of Krebs cycle metabolism using hyperpolarized ^{13}C magnetic resonance spectroscopy. FASEB J 23:2529-2538.

Schroeder MA, Lau AZ, Chen AP, Gu Y, Nagendran J, Barry J, Hu X, Dyck JR, Tyler DJ, Clarke K, Connelly KA, Wright GA, Cunningham CH (2013) Hyperpolarized $^{(13)}C$ magnetic resonance reveals early- and late-onset changes to in vivo pyruvate metabolism in the failing heart. Eur J Heart Fail 15:130-140.

Selvaraj S, Kelly DP, Margulies KB (2020) Implications of Altered Ketone Metabolism and Therapeutic Ketosis in Heart Failure. Circulation 141:1800-1812.

Shulman GI, Rothman DL, Jue T, Stein P, DeFronzo RA, Shulman RG (1990) Quantitation of muscle glycogen synthesis in normal subjects and subjects with non-insulin-dependent diabetes by ^{13}C nuclear magnetic resonance spectroscopy. N Engl J Med 322:223-228.

Sowton AP, Griffin JL, Murray AJ (2019) Metabolic Profiling of the Diabetic Heart: Toward a Richer Picture. Front Physiol 10:639.

Stanley WC, Recchia FA, Lopaschuk GD (2005) Myocardial substrate metabolism in the normal and failing heart. Physiol Rev 85:1093-1129.

Timm KN, Apps A, Miller JJ, Ball V, Chong CR, Dodd MS, Tyler DJ (2018) Assessing the optimal preparation strategy to minimize the variability of cardiac pyruvate dehydrogenase flux measurements with hyperpolarized MRS. NMR Biomed 31:e3992.

Tougaard RS, Laustsen C, Lassen TR, Qi H, Lindhardt JL, Schroeder M, Jespersen NR, Hansen ESS, Ringgaard S, Botker HE, Kim WY, Stodkilde-Jorgensen H, Wiggers H (2021) Remodeling after myocardial infarction and effects of heart failure treatment investigated by hyperpolarized [1-(13) C]pyruvate magnetic resonance spectroscopy. Magn Reson Med.

University of California SF, Healthcare G (2010) Hyperpolarized Pyruvate Injection in Subjects With Prostate Cancer. In: https://ClinicalTrials.gov/show/NCT01229618.

University of California SF, American Cancer Society I, Institute NC, Imaging NIfB, Bioengineering (2016) Pilot Study of (MR) Imaging With Pyruvate (^{13}C) to Detect High Grade Prostate Cancer. In: https://ClinicalTrials.gov/show/NCT02526368.

Veech RL (2006) The determination of the redox states and phosphorylation potential in living tissues and their relationship to metabolic control of disease phenotypes. Biochem Mol Biol Educ 34:168-179.

Veech RL, Eggleston LV, Krebs HA (1969) The redox state of free nicotinamide-adenine dinucleotide phosphate in the cytoplasm of rat liver. Biochem J 115:609-619.

Veech RL, Guynn R, Veloso D (1972) The time-course of the effects of ethanol on the redox and phosphorylation states of rat liver. Biochem J 127:387-397.

Voros G, Ector J, Garweg C, Droogne W, Van Cleemput J, Peersman N, Vermeersch P, Janssens S (2018) Increased Cardiac Uptake of Ketone Bodies and Free Fatty Acids in Human Heart Failure and Hypertrophic Left Ventricular Remodeling. Circ Heart Fail 11:e004953.

Wang ZJ, Ohliger MA, Larson PEZ, Gordon JW, Bok RA, Slater J, Villanueva-Meyer JE, Hess CP, Kurhanewicz J, Vigneron DB (2019) Hyperpolarized (13)C MRI: State of the Art and Future Directions. Radiology 291:273-284.

Whitbread AK, Masoumi A, Tetlow N, Schmuck E, Coggan M, Board PG (2005) Characterization of the omega class of glutathione transferases. Methods Enzymol 401:78-99.

Williamson JR, Jones EA (1964) Inhibition of glycolysis by pyruvate in relation to the accumulation of citric acid cycle intermediates in the pefused rat heart. Nature 203:1171-1173.

Wu CY, Satapati S, Gui W, Wynn RM, Sharma G, Lou M, Qi X, Burgess SC, Malloy C, Khemtong C, Sherry AD, Chuang DT, Merritt ME (2018) A novel inhibitor of pyruvate dehydrogenase kinase stimulates myocardial carbohydrate oxidation in diet-induced obesity. J Biol Chem 293:9604-9613.

Yoshihara HA, Bastiaansen JA, Berthonneche C, Comment A, Schwitter J (2015) An intact small animal model of myocardial ischemia-reperfusion: Characterization of metabolic changes by hyperpolarized ^{13}C MR spectroscopy. Am J Physiol Heart Circ Physiol 309:H2058-2066.

Yoshihara HAI, Bastiaansen JAM, Karlsson M, Lerche MH, Comment A, Schwitter J (2020) Detection of myocardial medium-chain fatty acid oxidation and tricarboxylic acid cycle activity with hyperpolarized [1-$^{(13)}C$]octanoate. NMR Biomed 33:e4243.